Science Advances
AAAS

advances.sciencemag.org/cgi/content/full/6/6/eaav7504/DC1

Supplementary Materials for

Chemokine receptor 4 targeted protein MRI contrast agent for early detection of liver metastases

Shanshan Tan, Hua Yang, Shenghui Xue, Jingjuan Qiao, Mani Salarian, Khan Hekmatyar, Yuguang Meng, Rao Mukkavilli, Fan Pu, Oluwatosin Y. Odubade, Wayne Harris, Yan Hai, Melinda L. Yushak, Vanessa M. Morales-Tirado, Pardeep Mittal, Phillip Z. Sun, David Lawson, Hans E. Grossniklaus, Jenny J. Yang*

*Corresponding author. Email: jenny@gsu.edu

Published 7 February 2020, *Sci. Adv.* **6**, eaav7504 (2020)
DOI: 10.1126/sciadv.aav7504

This PDF file includes:

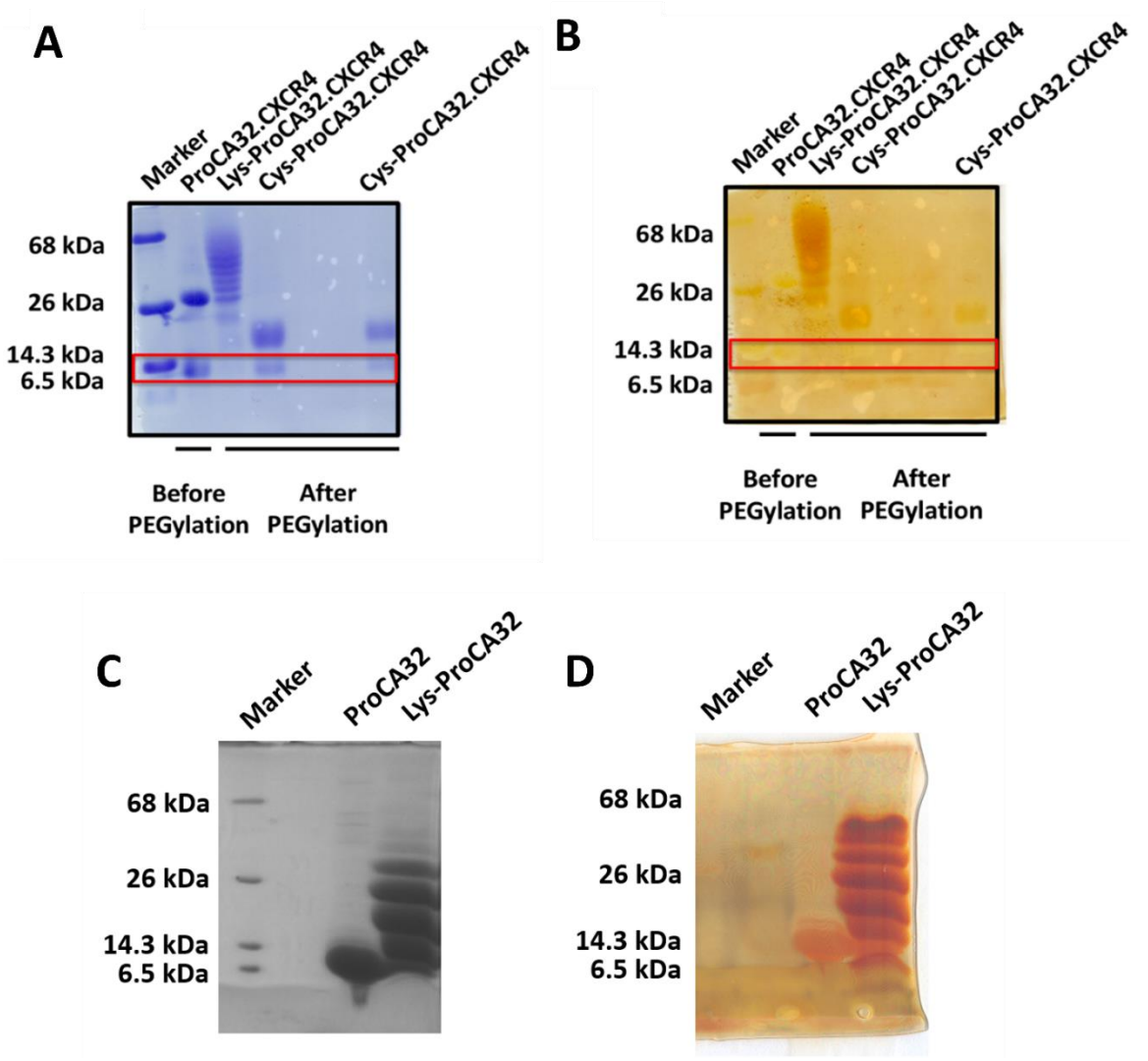

Fig. S1. PEGylation SDS-PAGE gel of protein contrast agents. (**A**) Coomassie blue staining of ProCA32.CXCR4 before and after PEGylation. Cysteine PEGylation of ProCA32.CXCR4 yield Cys-ProCA32.CXCR4 with one PEGylation site. Lysine PEGylation of ProCA32.CXCR4 yield Lys-ProCA32.CXCR4 with various numbers of PEGylation sites, indicated by the multiple protein bands after lysine PEGylation. (**B**) Iodine (I_2) staining of ProCA32.CXCR4 before and after PEGylation. Iodine staining identified PEG as brown color on SDS-PAGE gel, indicating the positions of PEGylated ProCA32.CXCR4. (**C**) Coomassie blue staining of ProCA32 before and after Lys-PEGylation. Multiple protein bands after Lys-PEGylation represent Lys-ProCA32 with various PEGylation sites. (**D**) Iodine staining of ProCA32 before and after Lys-PEGylation.

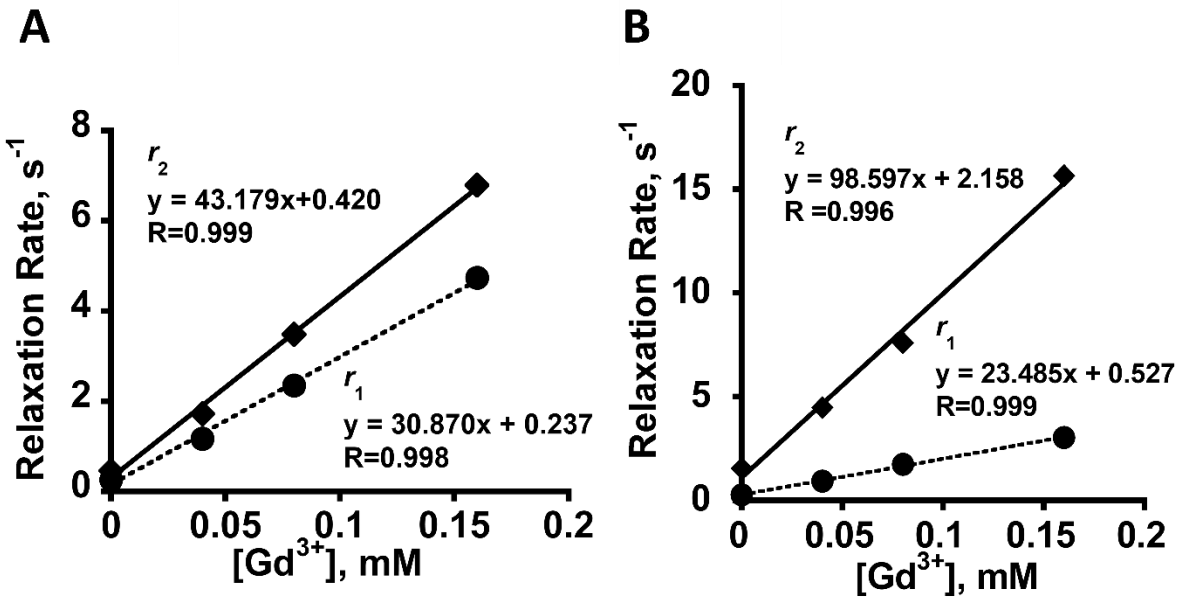

Fig. S2. Determination the relaxivity values of ProCA32.CXCR4. (**A**) Relaxivity assessment of ProCA32.CXCR4 with 60 MHz relaxometer. (**B**) Relaxivity assessment of ProCA32.CXCR4 with 7.0 T MRI scanner. The slopes of the lines represent the relaxivities of ProCA32.CXCR4.

A

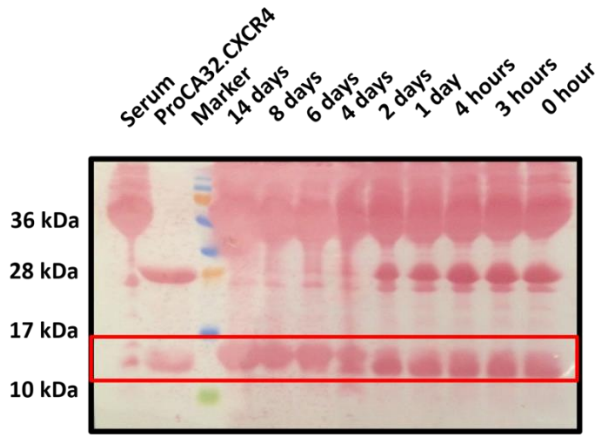

B

Contrast Agent	*Thermodynamic Index (R1t = 4320 min/R0t = 0 min)
ProCA32.CXCR4	0.96
Gadovist	0.95
ProHance	0.93
Dotarem	0.93
Eovist	0.91
MultiHance	0.82
Magnevist	0.72
Omniscan	0.39

Fig. S3. Serum stability and transmetalation study of ProCA32.CXCR4. (**A**) Ponceau-S staining of serum and ProCA32.CXCR4 mixture; pink bands indicate protein. ProCA32.CXCR4 is stable up to 14 days when incubated with serum at 37°C. ProCA32.CXCR4 is highlighted by the red square frame. (**B**) Transmetalation study of ProCA32.CXCR4. ProCA32.CXCR4 is inert towards Zn^{2+}; the thermodynamic index of ProCA32.CXCR4 is 0.96 after incubation with $ZnCl_2$ for 4320 min, whereas for ProHance it was 0.93, and 0.93 for Dotarem.

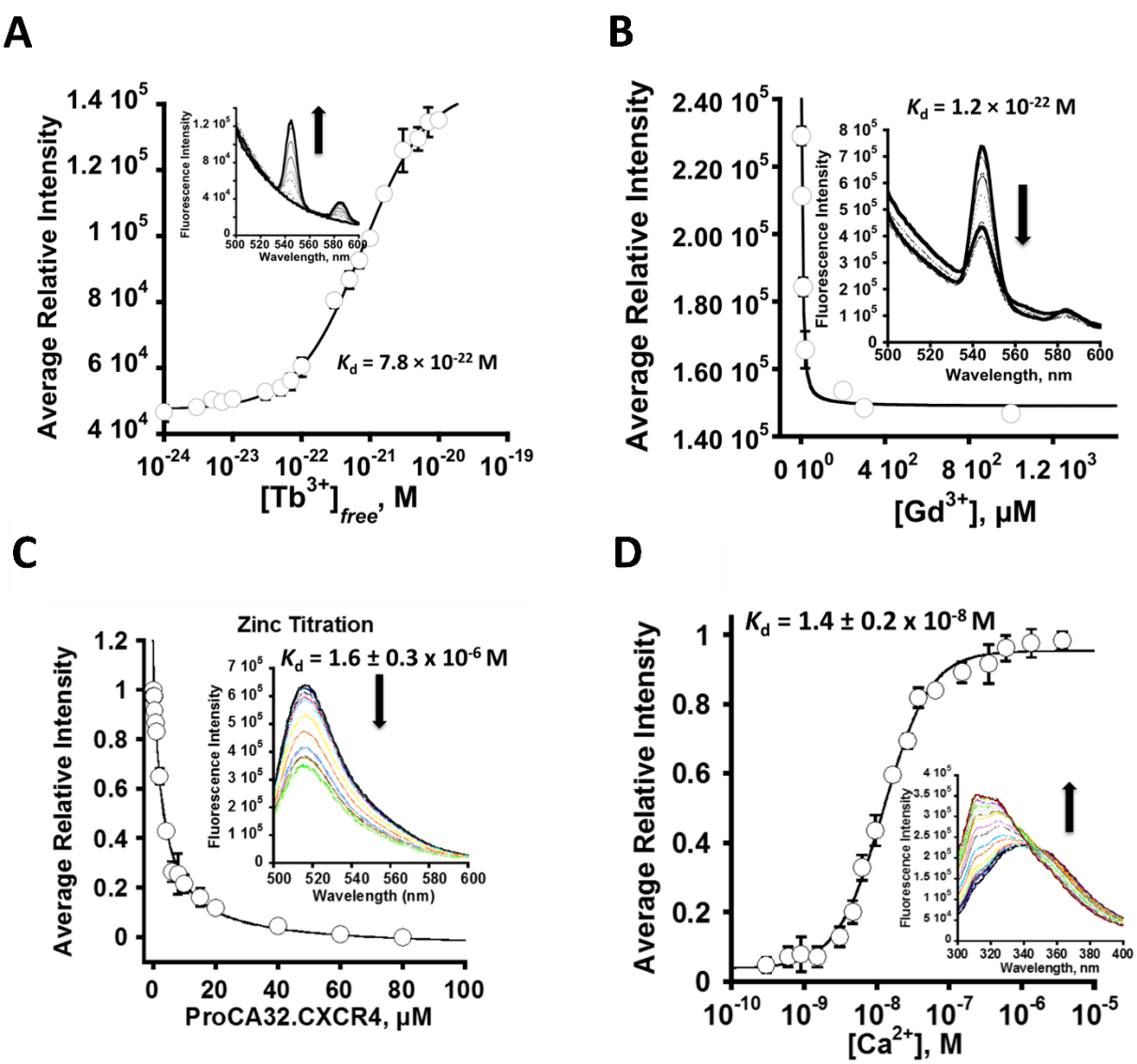

Fig. S4. Determination of ProCA32.CXCR4 metal binding affinities. (**A**) Determining the Tb^{3+} binding affinity of ProCA32.CXCR4. The K_d of Tb^{3+} binding to ProCA32.CXCR4 is 7.8×10^{-22} M. (**B**) Determining the Gd^{3+} binding affinity of ProCA32.CXCR4 via Gd^{3+}-Tb^{3+} competition. The K_d of Gd^{3+} binding to ProCA32.CXCR4 is 1.2×10^{-22} M. (**C**) Determining the Zn^{2+} binding affinity of ProCA32.CXCR4. The K_d of Zn^{2+} binding to ProCA32.CXCR4 is 1.6×10^{-6} M. (**D**) Ca^{2+} titration with ProCA32.CXCR4 to determine the Ca^{2+} binding affinity of ProCA32.CXCR4. The K_d of Ca^{2+} binding to ProCA32.CXCR4 is 1.4×10^{-8} M.

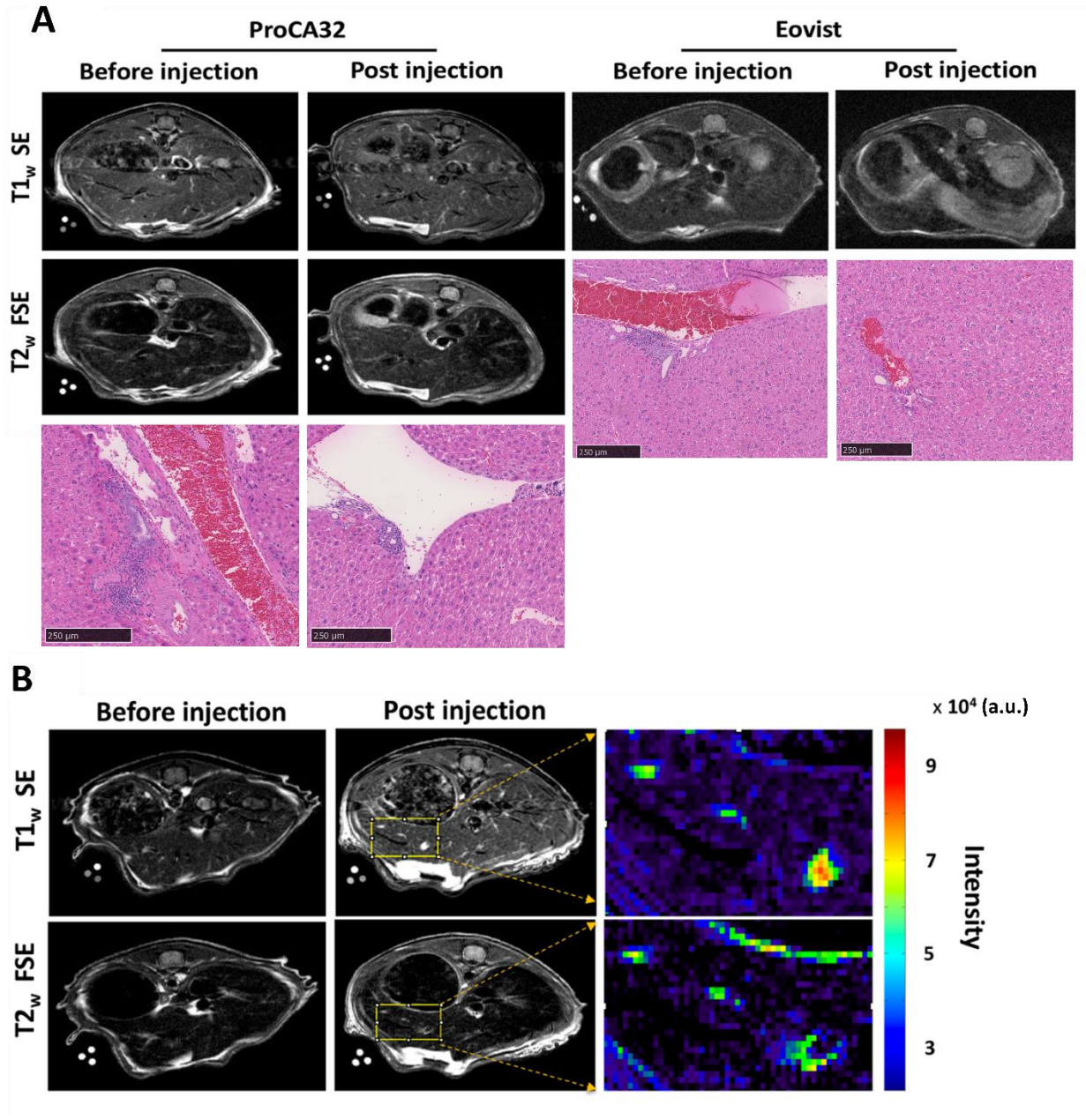

Fig. S5. MRI images of metastatic UM mice M20-09-196 before and after administration of Lys-ProCA32, Eovist, and Lys-ProCA32.CXCR4 (*n* = 2 for Eovist group, *n* = 3 for Lys-ProCA32 and Lys-ProCA32.CXCR4 group). (**A**) T_1-weighted spin echo, T_2-weighted fast spin echo MRI images of M20-09-196 mice before and after injection of Lys-ProCA32 and Eovist. H&E staining of corresponding mice are under the MRI images. No lesion enhancement was observed in MRI images at 48 h after Lys-ProCA32 injection as well as at 30 min after injection of Eovist. Histological analysis showed that both the mice with Lys-ProCA32 and Eovist injection have metastases in the liver. (**B**) T_1-weighted spin echo and T_2-weighted fast spin echo MRI images of M20-09-196 mice before and after injection of Lys-ProCA32.CXCR4. At 48 h

post-injection of Lys-ProCA32.CXCR4, three lesions were observable in both T_1- and T_2-weighted MRI images. Color heat map shows zoom-in view of metastases.

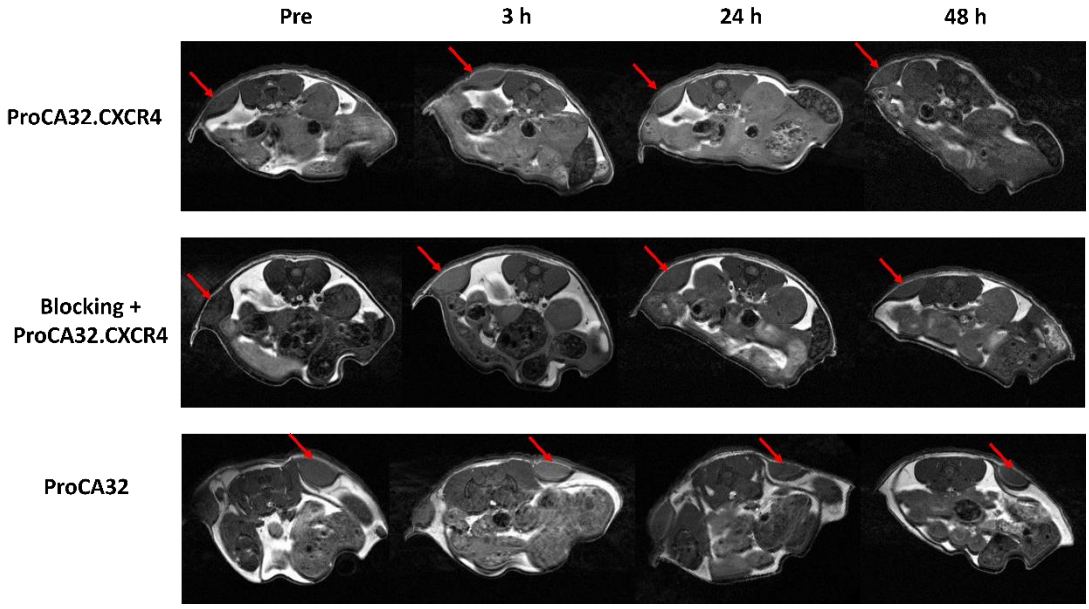

Fig. S6. T_1-weighted MRI images of subcutaneous UM mice before and after administration of Cys-ProCA32.CXCR4, blocking reagent + Cys-ProCA32.CXCR4, and Lys-ProCA32 (*n* = 3 for each group). Tumors are identified by red arrows. Three groups of mice exhibited tumor signal intensity increases at 3 h after injection of contrast agents. Mice that received injection of Cys-ProCA32.CXCR4 presented further tumor signal enhancement at 24 h after injection, and signal intensity then washed out at 48 h. CXCR4 blocking reagent pre-treated mice and Lys-ProCA32 administration showed signal wash out at 24 h and a further decrease at 48 h.

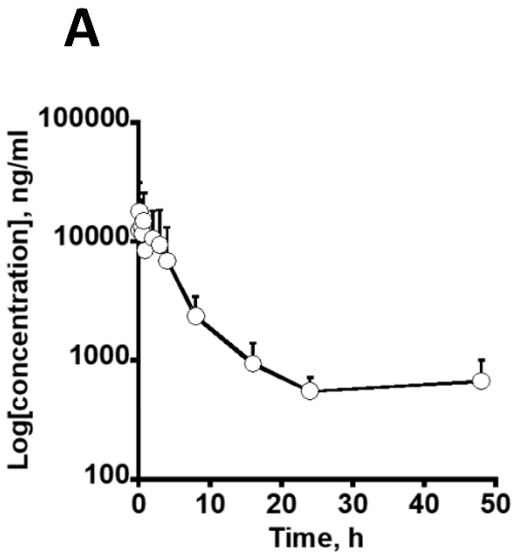

Contrast Agent	Eovist	Cys-ProCA32.CXCR4
$t_{1/2\beta}$ (h)	0.2	9.19
V_c (L/kg)	N/A	1.38
V_{ss} (L/kg)	0.21	1.96
CL (mL/min/kg)	0.4	0.31
MRT (h)	N/A	19.58
$AUC_{0\text{-}72h}$ (μg·h/mL blood)	N/A	113.20

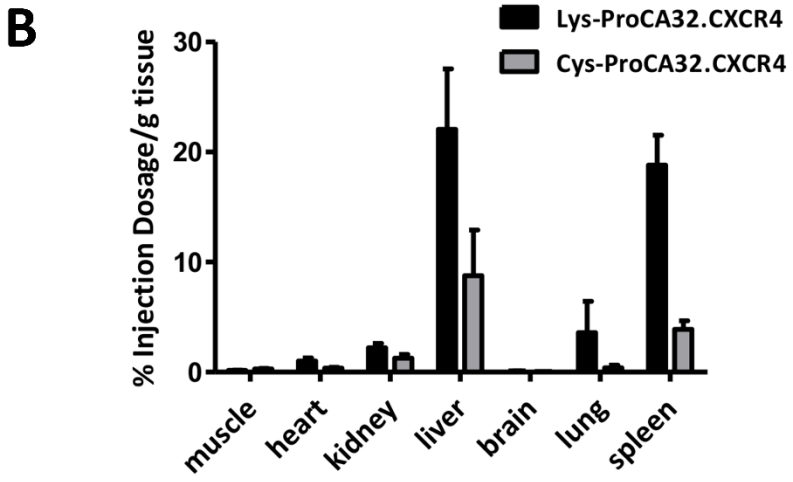

Fig. S7. Pharmacokinetic study of Cys-ProCA32.CXCR4 and ICP-OES analysis of Gd^{3+} content in different mouse organs. (**A**) Pharmacokinetics study of Cys-ProCA32.CXCR4 and in comparison with Eovist. Experiment details and abbreviation see material and method, pharmacokinetics study section. (**B**) ICP-OES analysis of Gd^{3+} content in different mouse organs. Mice (n = 3) organs, including muscle, heart, kidney, liver, brain, lung, and spleen, were collected five days after injection of 0.035 mmol/kg of either Lys-ProCA32.CXCR4 or Cys-ProCA32.CXCR4. Organs with the most Gd^{3+} distribution were the liver and spleen. Low amounts of Gd^{3+} were found in brain (0.07 % Injection Dosage/g tissue), muscle, and heart tissues. Moderate concentration of Gd^{3+} were found in both kidney and lung tissues.

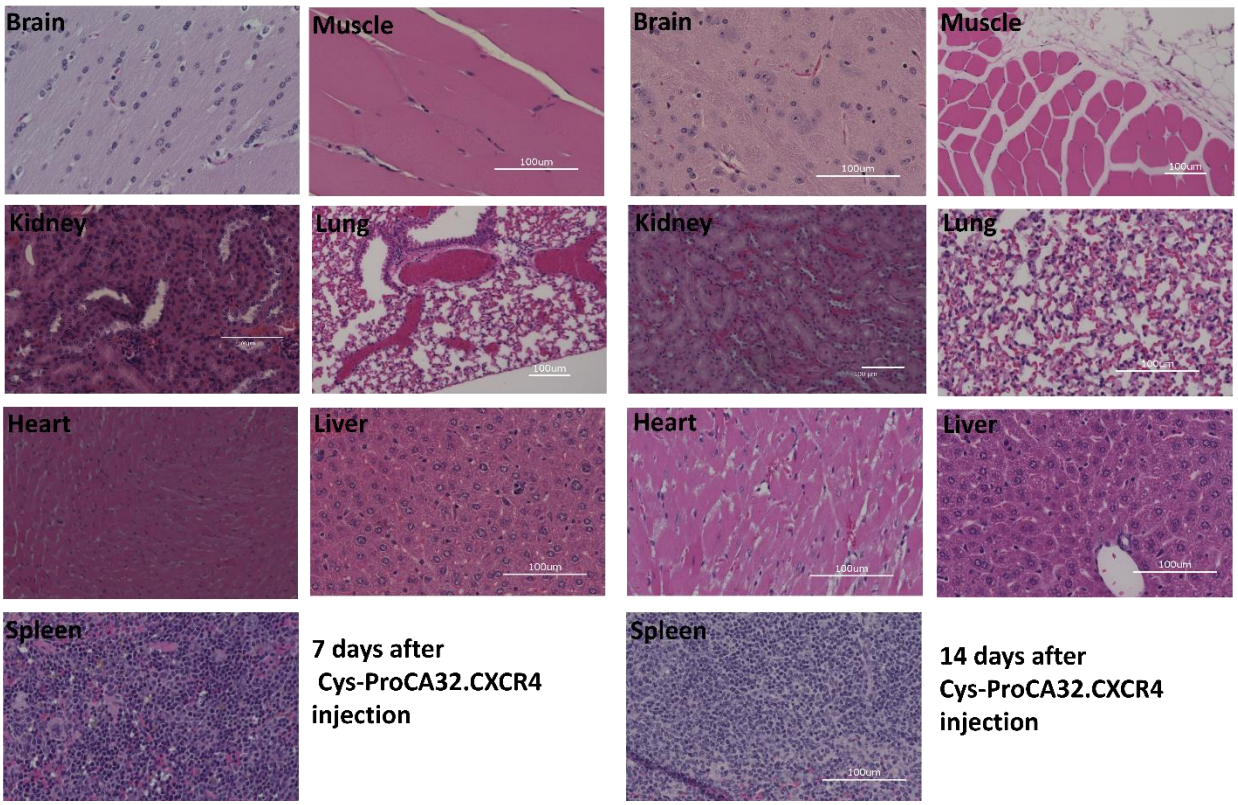

Fig. S8. H&E staining analysis of mice tissues collected 7 and 14 days after injection of Cys-ProCA32.CXCR4. Mice (n=3) organs, including brain, kidney, heart, spleen, muscle, lung, and liver were collected 7 and 14 days after injection of 0.035 mmol/kg Cys-ProCA32.CXCR4. No observable tissue damage occurred in the mouse organs.

Table S1. Relaxivities of investigated contrast agents in 10 mM Hepes at 37°C.

Relaxivities of investigated contrast agents in 10 Mm HEPES buffer at 37 °C				
Contrast agent	*r*1 (1.5 T)	*r*2 (1.5 T)	*r*1 (7.0 T)	*r*2 (7.0 T)
Dotarem®	3.0 ± 0.2	3.3 ± 0.4	2.8 ± 0.4	5.3 ± 0.5
Magnevist®	3.1 ± 0.4	3.3 ± 0.2	3.1 ± 0.4	6.7 ± 0.4
Eovist®	4.3 ± 0.5	5.4 ± 0.4	4.9 ± 0.1	7.8 ± 0.7
ProHance®	3.4 ± 0.6	3.3 ± 0.4	3.4 ± 0.1	8.3 ± 0.6
ProCA32.CXCR4	30.9 ± 0.5	43.2 ± 1.0	23.5 ± 1.2	98.6 ± 3.2
Lys-ProCA32.CXCR4	27.6 ± 0.9	41.4 ± 2.7	20.3 ± 1.1	93.7 ± 4.2
Cys-ProCA32.CXCR4	28.3 ± 0.6	40.2 ± 0.3	17.4 ± 0.7	88.7 ± 3.1

* Relaxivity values in $mM^{-1}\ s^{-1}$

Table S2. Clinical pathology profile of mouse serum. Mouse serum samples collected 2 days after injection of saline (control, n = 3) or 0.025 mmol/kg of Lys-ProCA32.CXCR4/Cys-ProCA32.CXCR4 (n = 3) were used for pathology profiling. Data are expressed as mean ± SD.

Analyte	Control	Lys-ProCA32.CXCR4	Cys-ProCA32.CXCR4
Cholesterol, mg/dL	98.3 ± 20.1	109.7 ± 26.4	110.3 ± 12.7
Glucose, mg/dL	283.0 ± 45.6	253.7 ± 92.0	282.0 ± 81.1
Calcium, mg/dL	11.0 ± 0.5	7.6 ± 2.1	9.4 ± 0.5
Phosphorus, mg/dL	12.8 ± 1.5	13.7 ± 3.0	13.8 ± 3.5
Chloride, mmol/L	110.1 ± 5.1	104.7 ± 4.2	109.2 ± 7.3
Potassium, mmol/L	12.6 ± 0.7	10.4 ± 0.9	15.7 ± 3.3
Sodium, mmol/L	149.2 ± 4.7	144.0 ± 5.6	141.5 ± 2.5
Creatinine, mg/dL	0.2 ± 0.1	0.4 ± 0.3	0.6 ± 0.5
Albumin, g/dL	3.0 ± 0.3	2.9 ± 0.5	3.1 ± 0.3
Total Bilirubin, mg/dL	0.2 ± 0.2	0.4 ± 0.3	0.3 ± 0.2
ALP(U/L)	85.7 ± 13.3	52.3 ± 18.6	46.3 ± 18.9
ALT(U/L)	36.0 ± 7.9	74 ± 9.2	118.0 ± 31.7